EXPERIMENTAL STUDY OF THE DRAG OF A TWO-PHASE HELIUM FLOW IN CHANNELS

I. P. Vishnev, L. N. Migalinskaya,
and I. B. Lebedeva

UDC 532.529.5

Results are presented from an experimental study of the drag of a turbulent two-phase helium flow in a horizontal channel under adiabatic conditions.

In engineering practice, the drag of two-phase flows is usually calculated using relations based on models of separate and homogeneous flow:

$$\frac{\Delta P_{\text{tp}}}{\Delta P'_{\text{sp}}}=(1-x)^{1.75}\Phi^2,\ \Phi^2=f(\chi),$$

where

$$\chi=\left(\frac{\rho''}{\rho'}\right)^{0.5}\left(\frac{\mu'}{\mu''}\right)^{0.125}\left(\frac{1}{x}-1\right)^{0.875}; \tag{1}$$

$$\frac{\Delta P_{\text{tp}}}{\Delta P'_{\text{sp}}}=\left[1+x\left(\frac{\rho'}{\rho''}-1\right)\right]\left[1+x\left(\frac{\mu'}{\mu''}-1\right)\right]^{-0.25}. \tag{2}$$

These relations were obtained by systematic analysis of the results of experiments on air–water or steam–water mixtures and are empirical or semiempirical in nature [1, 2]. The feasibility of using them to calculate the drag of a two-phase helium flow requires experimental confirmation.

Figure 1 compares these relations with respect to the drag of two-phase flows calculated from helium parameters at a pressure $P = 1.2\cdot10^5$ Pa. It can be seen that the relations differ by a factor greater than four in the region of moderate vapor contents.

Several experimental studies of the drag of a two-phase helium flow in channels have been published [3-6]. The experimental data in [5, 6] are the most interesting. It was obtained from measurement of the resistance of a two-phase helium flow in a vertical channel. There have been almost no studies of the structure of two-phase helium flows, while the effect of flow conditions in two-phase media on drag is widely known.

The scarcity of test data complicates the task of determining the suitability of this or that relation for calculating the drag of two-phase helium. This problem could be solved on the basis of more extensive empirical data. The present work presents results of tests we conducted to determine the effect of the basic flow parameters of pressure P, mass flow-rate vapor content x, and mass velocity ρw on the drag and structure of a two-phase helium flow.

The helium flow was realized on a test stand in a thin-walled steel tube 6 × 0.4 mm in diameter with a total length of 3000 mm. The tube was enclosed in an insulated jacket [7]. The use of highly efficient vacuum-laminated insulation of PÉTF-0.01 polyethyleneterphthalate film with interlayers of SBR-40 glass paper in the experimental pipe significantly reduced heat inflow from the environment and created test conditions which approached adiabatic conditions as closely as possible.

The structure of the flow was observed by making a section of the pipe out of vacuum-tight molybdenum glass, similar to a Dewar flask. An initial vacuum of the order of 0.133 Pa was maintained in the space between the walls. The model (the glass section of the pipe) was butt-joined with the rest of the pipe with a vacuum rubber seal.

All-Union Scientific-Research Institute of Helium Engineering, Moscow. Translated from Inzhenerno-Fizicheskii Zhurnal, Vol. 43, No. 2, pp. 195-201, August, 1982. Original article submitted May 7, 1981.

0022-0841/82/4302-0841$07.50

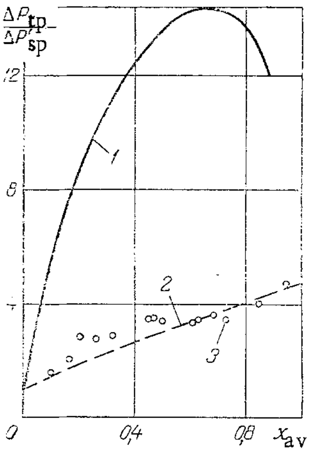

Fig. 1

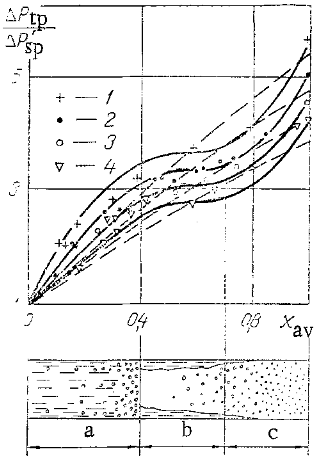

Fig. 2

Fig. 1. Comparison of calculated curves of the resistance of a two-phase flow with test data for two-phase helium at $P = 1.2 \cdot 10^5$ Pa: 1) theoretical curve of Martinelli; 2) theoretical curve of homogeneous-flow model; 3) test data of authors.

Fig. 2. Curve of change in relative resistance of a two-phase helium flow $\Delta P_{tp}/\Delta P'_{sp}$ and flow structure relative to mass vapor content x_{av} under adiabatic conditions for different pressures: 1) $P = 1.1 \cdot 10^5$ Pa; 2) $1.2 \cdot 10^5$; 3) $1.3 \cdot 10^5$; 4) $1.4 \cdot 10^5$; a) bubble regime of flow; b) annular regime; c) disperse regime.

The tests were conducted at constant pressures and mass velocities. The inlet vapor content of the two-phase mixture was measured in each series of tests. The ranges of the flow parameters were: $1 \cdot 10^5$ to $1.4 \cdot 10^5$ Pa pressure, 65 to 400 kg/m^2·sec mass velocity, and 0 to 1 mass vapor content.

The required composition of two-phase mixture was created by evaporating part of the liquid with an electric heater installed at the inlet section of the pipe. The pressure drop of the two-phase helium flow was measured in a 1200-mm-long section of the pipe. Pressure was sampled here with special annular chambers which were connected by four 0.4-mm-diameter holes with the internal cavity of the pipe. Thermal and hydrodynamic stabilization sections 1500 and 300 mm long, respectively, were located before and after the measurement section. Each test series entailed measurement of the pressure and temperature at the pipe inlet, the pressure drop in the measurement section of the pipe, the flow rate of evaporated helium and the level of liquid in the container, and the power of the load delivered to the electric heater. Analysis of the errors showed that the maximum error was obtained in determining helium flow rate and amounted to 7.8%.

The drag of the two-phase flow was determined as the difference between the pressure drop measured in the measurement section of the pipe and the calculated pressure loss due to acceleration of the flow:

$$\Delta P_{tp} = \Delta P_{expt} - \Delta P_{acc}. \tag{3}$$

Since there are no literature data on actual volume vapor contents of two-phase helium, the pressure loss due to flow acceleration was calculated using the flow-rate vapor content, i.e.,

$$\Delta P_{acc} = \frac{(\rho w)^2}{\rho'}\left(\frac{\rho'}{\rho''} - 1\right)(x_2 - x_1). \tag{4}$$

The mass flow-rate vapor content of the flow was calculated from the heat-balance equation with the known parameters of the helium at the pipe inlet. The theoretical equation appears as follows when solved for the vapor content x for any section z of the pipe:

TABLE 1. Test Data on the Drag of a Two-Phase Helium Flow in a Horizontal Channel, d = 5.2 mm, l = 1200 mm

№	$P\cdot 10^{-5}$, Pa	ρw, kg/m^2·sec	N, W	x_{av} %	ΔP_{expt}, Pa
		$P = 1{,}1\cdot 10^5$ Pa			
1	1,103	85	5,7	13,62	230
2	1,103	85	7,6	19,0	240
3	1,07	113	4,23	7,2	280
4	1,11	110	7,6	14,6	300
5	1,11	110	7,7	15,0	350
6	1,1	325	22	14,3	3200
7	1,1	345	25	18,1	2700
8	1,13	285	3,7	1,45	1100
9	1,15	120	5,8	11,0	500
10	1,15	190	7,95	8,84	600
11	1,16	75	5,8	17,6	220
12	1,162	75,3	13,8	42,9	300
13	1,162	76	13,75	42,5	290
14	1,16	80	2,38	7,2	142
15	1,16	80,5	4,5	13,6	199
16	1,16	81	4,88	14,75	188
17	1,16	82	3,8	11,45	204,5
18	1,16	82	5,83	17,6	234
19	1,16	80	9,74	29,4	275
20	1,16	80	12,75	38,5	309
21	1,16	78	12,43	37,55	282,5
22	1,16	80	14,2	42,9	322,5
23	1,16	81	16,9	51	333
24	1,16	80	22,2	67	356
25	1,16	82	24,85	75	386
26	1,16	79	26,8	81	404
27	1,16	112	18,23	38,5	520
		$P = 1{,}2\cdot 10^5$ Pa			
28	1,21	70	20	72,5	285
29	1,205	72	25	83,9	340
30	1,2	72,5	22	78,5	330
31	1,21	78	23	80	389
32	1,19	80	22,2	76,7	420
33	1,2	82,5	21	73,5	400
34	1,21	87	18,3	63,4	450
35	1,21	80	23,3	58,2	415
36	1,205	101	20	49,25	450
37	1,2	106	21	52,9	350
38	1,22	106,5	19	46,8	480
39	1,21	108	19,1	47	450
40	1,2	110	17	41,4	370
41	1,205	113	17,9	45,5	550
42	1,205	114	20,5	51,5	530
43	1,21	122	4,95	10,0	290
44	1,2	121	8,15	16,3	405
45	1,2	120	8,52	17,4	464
46	1,21	120,5	14,4	29,4	557
47	1,205	122	18,75	38,2	577
48	1,205	121	18,9	38,5	622
49	1,19	120	22,15	45,2	632
50	1,20	119	23,1	47	632
51	1,21	120	25,5	52	622
52	1,22	121	28	57,1	652
53	1,2	120,5	29,4	60	652
54	1,2	119	30,4	62,1	662
55	1,21	122	36,3	74,1	695
56	1,2	121	38,7	79,9	721
57	1,21	120	39,65	81,2	793
58	1,21	119	41,1	84,05	780
59	1,22	123	44,7	91,5	689
60	1,2	120	45,5	93,1	918
61	1,21	142	25,1	42	1010
62	1,21	149	25,2	40	1115

TABLE 1 (Continued)

№	$P\cdot 10^{-5}$, Pa	ρw, kg/m$^2\cdot$sec	N, W	x_{av}, %	ΔP_{expt}, Pa
		$P = 1{,}3\cdot 10^5$ Pa			
63	1,31	71,5	17,2	48,5	258
64	1,3	72	26,2	99,5	400
65	1,31	80	24,6	76,7	420
66	1,32	89	21	61,3	450
67	1,32	91	20,5	60,5	470
68	1,31	100	1,22	3,0	177,3
69	1,28	102	10,6	27	423
70	1,3	100	12,6	31,9	431,5
71	1,3	101	20,3	51,5	498
72	1,31	101	23,85	60,6	517,5
73	1,31	100	28,9	73,5	556
74	1,33	99	38,5	97,9	735
		$P = 1{,}4\cdot 10^5$ Pa			
75	1,4	130	29	56,5	725
76	1,41	134	26,5	41,6	800
77	1,4	140	4,75	9,0	414
78	1,41	141	9,23	17,5	488
79	1,38	140	10,75	20,1	413
80	1,4	139	13,62	25,85	620
81	1,39	140	16	30	739
82	1,41	141	17,1	32,1	724
83	1,41	142	16,9	32	680
84	1,4	140	18,95	36	768
85	1,4	140,5	22,1	42	848
86	1,42	140	29,6	56	827
87	1,39	141	31,7	60,1	812,5
88	1,4	140	34,3	65,0	887
89	1,4	142	43,5	82,5	1000
90	1,41	139	47,4	89,9	1093
91	1,41	140	50,7	96,15	1211
92	1,42	145	36,5	73,6	1335
93	1,4	148	20,8	31	870
94	1,39	195	34	36,75	1600
95	1,4	196	32,8	36,6	1580
96	1,4	224	16,1	20,1	1330
97	1,41	224	27	32	1590
98	1,41	227	20	25,75	2180
99	1,4	263	36	52,45	2700

$$x = x_0 + \frac{N}{Gr} + \frac{q_{en}z}{Gr} + \int_{P_1}^{P_2} \frac{di_p}{r} + \int_{P_1}^{P_2} \frac{v_{mx}\,dP}{427r}. \tag{5}$$

Analysis of the components of Eq. (5) showed that the maximum change in vapor content resulting from the total heat release through isentropic expansion $\int_{P_1}^{P_2} \frac{di_p}{r}$ and the action of friction $\int_{P_1}^{P_2} \frac{v_{mx}\,dP}{427r}$ in the pipe is no more than 1%. The addition of heat to the flow from the environment $q_{en.}a/Gr$ is also slight ($q_{en.}$ = 0.12 W/p·m) and changes vapor content by about 2% at low flow rates of the working medium (ρw < 80 kg/m^2·sec). Thus, in calculating flow-rate vapor content, we can ignore the effect of these three components of Eq. (5) and, within the limits of the error in the variation of the basic flow parameters, assume that the flow of the medium is adiabatic.

Table 1 shows the resulting test data on the resistance of the two-phase helium flow. Figure 2 shows experimental results in the form of ratios of pressure drops for single- and two-phase helium flows, with the same mass flow rate, versus the vapor content [8]. The same figure shows data for a mass velocity ρw = 120 kg/m^2·sec at different pressures. Mass velocity was not seen to have had an effect on the resistance of the flow in the investigated velocity range. The dashed lines show theoretical curves for the homogeneous-flow model. It can be seen that the empirical data are stratified with respect to pressure, with an increase in the latter being accompanied by a decrease in the relative resistance of the two-phase mixture.

Comparison of the test data with the calculated data for homogeneous flow showed that the empirical points deviate somewhat from the theoretical curve, first being above, then below the latter. Meanwhile, the deviation is greater, the lower the pressure of the mixture. The deviation is 35-45% in the investigated pressure range. Such a complicated dependence of relative resistance $\Delta P_{tp}/P'_{sp}$ on mass vapor content can be explained by a change in the structure of the two-phase helium flow. Three sections with different slopes are evident on the empirical curve, these sections corresponding to different flow regimes. Visual observations established that the first section, for $x < 0.4$, corresponds to the bubble flow regime. This gradually changes to the emulsive regime. The second, transitional section of the curve, at vapor contents $x = 0.4$-0.7, corresponds to the annular flow regime. Here, all of the liquid moves in the form of a thin film over the walls of the pipe. Finally, the third section, for $x > 0.7$, corresponds to the disperse regime. Here, the liquid remaining in the form of fine droplets is distributed throughout the vapor flow.

The abrupt increase in the drag of the two-phase flow on the first and third sections of the curve is attributable to a rapid increase in the number of tiny vapor bubbles in the liquid or the number of liquid droplets in the vapor flow and, hence, to an increase in the size of the phase boundary. The presence of these disperse particles, having a large phase contacting surface and undergoing relatively little surface deformation themselves, leads to an increase in drag. The different slopes of the curve sections is attributable to the different compressibilities and deformabilities of the vapor bubbles and liquid droplets, their different drags and the differing curvatures of their paths. The weak dependence of drag on vapor content in the annular regime is due to the presence of a distinct phase boundary whose surface area changes little with vapor content. Here, the vapor occupies almost the entire cross section of the channel ($0.75 < \beta < 0.95$), while the liquid phase moves over the walls in the form of a film. The thickness of this film decreases with an increase in vapor content, which leads to some increase in the surface area of the phase boundary and drag.

By analogy with the processes which occur in the motion of a high-pressure vapor—water mixture [9], the shift in flow structure for the regimes we observed is accompanied by hydrodynamic crises. The first crisis occurs at vapor contents $x = 0.38$-0.42, while the second takes place at $x = 0.7$-0.75. With an increase in pressure, the crisis zone shifts somewhat toward lower vapor contents.

Comparison of the test data on the resistance of a two-phase helium flow in the pressure range $P = 1$-$1.8 \cdot 10^5$ Pa ($P/P_{cr} = 0.44$-0.8) in vertical and horizontal channels with approximate theoretical relations for models of separate and homogeneous flow of the phase (Fig. 1) showed that the homogeneous-flow model more closely (to within ±35-55%, depending on the pressure) describes the experimental data on drag in the flow of two-phase helium in channels.

NOTATION

d, diameter, m; G, mass flow rate, kg/sec; l, length, m; N, power of electric heater, W; P, pressure, Pa; ΔP, pressure drop, Pa; q, heat flux, W/p·m; r, latent heat of vaporization, J/kg; w, velocity, m/sec; ρw, mass velocity, $kg/m^2 \cdot sec$; x, mass flow-rate vapor content; β, volume flow-rate vapor content; μ, absolute viscosity, Pa·sec; ρ, density, kg/m^3. Indices: ', ", values of quantities for liquid or vapor, respectively, on the saturation line; in, out, values of quantities at the channel inlet or outlet; tp, two-phase; sp, single-phase; cr, critical; en., environment; mx, mixture; acc, acceleration; expt, experimental.

LITERATURE CITED

1. S. S. Kutateladze and M. A. Styrikovich, Hydrodynamics of Gas—Liquid Systems [in Russian], Énergiya, Moscow (1976).
2. G. Hollis, Unidimensional Two-Phase Flows [Russian translation], Mir, Moscow (1972).
3. V. E. Keilin, E. Klimenko, and I. Kovalev, "Device for measuring pressure drop and heat transfer in two-phase helium flow," Cryogenics, 9, No. 1, 36-38 (1969).
4. A. de La Harpe, Lehongre, I. Mollard, and C. Iohannes, "Boiling heat transfer and pressure drop of liquid helium-1 under forced circulation in a helically coiled tube," Adv. Cryog. Eng., 14, 170-177 (1969).

5. V. I. Deev, Yu. V. Gordeev, and A. I. Pridantsev, "Drag in the forced movement of a two-phase helium flow in channels," At. Energ., 42, 339-340 (1977).
6. B. S. Petukhov, V. M. Zhukov, and V. M. Shil'dkret, "Experimental study of drag in flow in a vertical pipe," Teplofiz. Vys. Temp., 18, No. 5, 1040-1044 (1980).
7. I. P. Vishnev, A. I. Krauze, S. I. Sergeev, et al., "Study of heat exchange and the hydrodynamics of helium for cooling superconductors," Collection of Documents of the Conference: Equipping the Cryogenic Systems of Superconducting and Cryoresistive Electrical Transmission Lines and Machinery with Superconducting Windings, Bratislava, Czechoslovak Socialist Republic (1978), pp. 96-122.
8. I. P. Vishnev, Ya. G. Vinokur, O. A. Sedov, et al., "Study of certain questions on the boiling of helium," in: Sixth All-Union Conference on Two-Phase Flow in Elements of Power Plants and Machinery, Summary of Documents, TsKTI (Central Scientific-Research, Planning, and Design Institute of Boilers and Turbines), Leningrad (1978), pp. 75-77.
9. N. V. Tarasova, "Drag in the boiling of water and a steam-water mixture in heated pipes and annular channels," Tr. Tsentr. Nauchno-Issled. Proektno-Konstr. Kotloturbinnyi Inst., No. 59, 47-58 (1965).

EQUATION OF EQUILIBRIUM EMISSION AND RETARDATION PARAMETERS IN NUCLEAR-POWER-PLANT TURBINES WITH DISSOCIATING NITROGEN TETROXIDE

É. A. Orudzhaliev

UDC 621.039.534

The equation of emission, retardation parameters, and expressions for quantities at the flow crisis are obtained for the case of dissociating nitrogen tetroxide.

I. Equations of Gas Emission and Flow Rate

The most interesting of the prospective heat carriers and working media in nuclear power plants is dissociating nitrogen tetroxide, i.e., the dissociating system

$$N_2O_4 \rightleftarrows 2NO_2 \rightleftarrows 2NO + O_2.$$

In [1] expressions were obtained for the isentropic heat incidence in a nozzle network, at the working blades, and in the turbine, written respectively in the form

$$h_{\text{n.}l} = \frac{w_{1t}^2 - w_0^2}{2} = \frac{R}{\mu}\frac{k_T}{k_T - 1}\bar{\eta}T_0\left[1 - \left(\frac{p_1}{p_0}\right)^{(k_T-1)/k_T}\right] - \frac{R}{\mu}T_0[(Z_{1\text{ef}})_{T_0} - (Z_{0\text{ef}})_{T_0}], \tag{1}$$

$$(L_0)_{\text{w.b}} = \frac{R}{\mu}\frac{k_T}{k_T - 1}\bar{\eta}T_1\left[1 - \left(\frac{p_2}{p_1}\right)^{(k_T-1)/k_T}\right] - \frac{R}{\mu}T_1[(Z_{2\text{ef}})_{T_1} - (Z_{1\text{ef}})_{T_1}] - \frac{w_{2t}^2 - w_1^2}{2}, \tag{2}$$

$$H_0 = \frac{R}{\mu}\frac{k_T}{k_T - 1}\bar{\eta}T_0\left[1 - \left(\frac{p_2}{p_0}\right)^{(k_T-1)/k_T}\right] - \frac{R}{\mu}T_0[(Z_{2\text{ef}})_{T_0} - (Z_{1\text{ef}})_{T_0}]. \tag{3}$$

The quantity $(k_T - 1)/k_T$ appears in Eqs. (1)-(3). In [1], the following dependence was established

$$\omega = \frac{C_p}{R/\mu}\frac{k_T - 1}{k_T}. \tag{4}$$

For dissociating nitrogen tetroxide, Eq. (4) is written in the form

$$\frac{k_T - 1}{k_T} = \frac{R}{\mu_{N_2O_4}}\frac{\omega}{C_{p\,\text{ef}}}. \tag{5}$$

M. Azizbekov Azerbaidzhan Institute of Petroleum and Chemistry, Baku. Translated from Inzhenerno-Fizicheskii Zhurnal, Vol. 43, No. 2, pp. 201-209, August, 1982. Original article submitted March 30, 1981.

0022-0841/82/4302-0846$07.50